

HIGHER-ORDER DIFFERENCING FOR GEOTHERMAL RESERVOIR SIMULATION

Curtis M. Oldenburg and Karsten Pruess

Earth Sciences Division
Berkeley Lab
Berkeley, California, 94720

ABSTRACT

We have implemented total variation diminishing (TVD) higher-order differencing schemes for two-dimensional non-uniform grids in the multiphase and multicomponent reservoir simulator TOUGH2. Higher-order differencing may be more efficient in reducing numerical dispersion than grid refinement. Much existing work in the literature on higher-order differencing schemes has focused on one- and two-dimensional tracer transport using explicit formulations for the convection-dispersion equation. We find that higher-order differencing schemes can also increase the accuracy of component transport, phase transport, and thermal energy transport in strongly advective situations in an implicit and multicomponent framework such as that used in TOUGH2. We have verified our implementation of higher-order schemes in TOUGH2/EOS7R by comparison with an analytical solution. We further applied the method to a problem of reinjection into a geothermal reservoir and compared results calculated using the Leonard TVD scheme against full upstream weighting. Higher-order differencing schemes show promise for decreasing numerical dispersion and improving geothermal reservoir simulation.

INTRODUCTION

Reinjection into geothermal reservoirs can cause strong forced convection in reservoir fracture zones. An optimal reinjection scheme will maximize heat transfer from the reservoir rocks to the injected fluid, while avoiding premature thermal breakthrough at production wells. Estimates of thermal breakthrough can be made in the field by injecting fluids with chemical tracers and monitoring produced fluids. Tracer breakthrough occurs before thermal breakthrough due to the effects of thermal retardation. Predictions of tracer and thermal breakthrough can be made by numerical simulation. However, injection simulations with standard finite-difference techniques may erroneously predict early tracer breakthrough because of numerical dispersion effects, leading to an overly conservative injection design.

One way to decrease numerical dispersion is to refine the spatial discretization for the numerical simulation. However, execution times and computer memory requirements increase exponentially with finer discretizations and can become expensive. Another approach is the use of higher-order differencing schemes that use the same total number of grid blocks but achieve greater accuracy in strongly advective situations. With higher-order differencing, the order of the matrix defining the linear equations to be solved remains the same while the bandwidth increases. Nevertheless, memory and run time requirements per time step are only modestly greater using higher-order differencing for two-dimensional problems. The purpose of this paper is to describe our ongoing work implementing higher-order differencing schemes into the reservoir simulator TOUGH2 and to present verification and a preliminary application.

BACKGROUND

Finite difference methods for the advection-diffusion equation involve the approximation of quantities such as temperature, concentration, and saturation at interfaces between grid blocks in order to calculate fluxes. In strongly convective situations, these approximations can result in overly diffusive (i.e. too much) flux or oscillatory and non-physical values for the quantities near sharp fronts. These well-known problems have led to the development of flux-limiting and total variation diminishing (TVD) schemes (e.g., Sweby, 1984) which taken together can be called higher-order differencing schemes. In flux-limiting schemes, a small amount of anti-diffusive flux is added to compensate for the otherwise overly diffusive flux calculation. TVD refers to the variations in the system tending to smooth out or diminish with time. One scheme that has proven stable and very accurate is the Leonard TVD scheme (Leonard, 1984; Datta-Gupta et al., 1991). While the early schemes were developed for explicit time stepping and usually in one dimension, the use of higher-order differencing for implicit schemes in oil reservoir engineering in two (Blunt and Rubin, 1992)

and three dimensions (Liu et al., 1995) has recently been introduced. In this work, we continue the development of higher-order differencing for implicit schemes and focus on realistic two-dimensional systems with relevance to geothermal reservoir engineering.

MATHEMATICAL DEVELOPMENT

The essence of achieving accurate flux calculations is in the approximation of interface quantities. For the development presented below, we assume a generic advection-diffusion equation as the model equation and consider the advection of a solute of concentration C over a non-uniform grid in the direction left to right as shown in Fig. 1. We further assume the method is fully implicit, with all values of concentration taken at the current most recent iterative step.

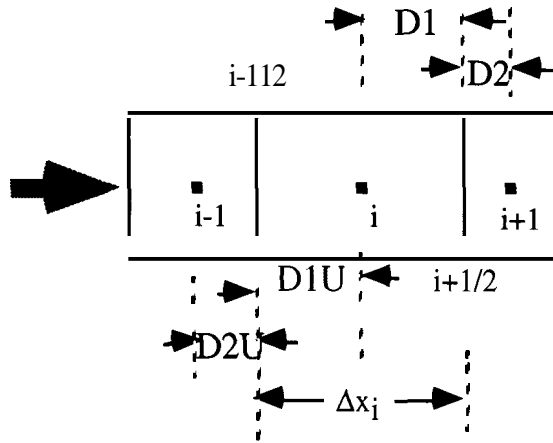


Fig. 1. Three non-uniform grid blocks with velocity from left to right. The standard TOUGH2 connection is between i and $i+1$ and has connection distances $D1$ and $D2$ and an interface at $i+1/2$. In higher-order schemes, we use the upstream grid block $i-1$ with connection distances $D1U$ and $D2U$ and the interface $i-1/2$.

We begin by writing an approximation for C at the $i+1/2$ interface as

$$C_{i+1/2} \approx C_i + D1 \left(\frac{C_{i+1} - C_i}{D1 + D2} \right) \quad (1)$$

which can be rearranged to

$$C_{i+1/2} \approx C_i + \frac{D1}{D1 + D2} (C_{i+1} - C_i) \quad (2)$$

Defining r , the ratio of upstream to downstream gradients, as follows,

$$r \equiv \frac{\left(\frac{\partial C}{\partial x} \right)_{i-1/2}}{\left(\frac{\partial C}{\partial x} \right)_{i+1/2}} = \frac{\left(\frac{C_i - C_{i-1}}{D1U + D2U} \right)}{\left(\frac{C_{i+1} - C_i}{D1 + D2} \right)} \quad (3)$$

and rearranging to

$$r \equiv \frac{D1 + D2}{D1U + D2U} \left(\frac{C_i - C_{i-1}}{C_{i+1} - C_i} \right) \quad (4)$$

we can propose that

$$C_{i+1/2} \approx C_i + \frac{D1}{D1 + D2} \Phi(r) (C_{i+1} - C_i) \quad (5)$$

where $\Phi(r)$ is a function of r . Depending on the function $\Phi(r)$, different approximations for the interface value $C_{i+1/2}$ can be made (see Table 1). For example, if $\Phi(r) = 0$, interface quantities are upstream weighted, a scheme which is always stable and standard in many reservoir simulators, but which leads to considerable numerical dispersion. If $\Phi(r) = 1$, a weighted average scheme results. In the non-trivial functions, limits (flux limiters) are set on $\Phi(r)$ to make the scheme TVD, precluding spurious oscillations and instability. TVD values of $\Phi(r)$ are plotted in the shaded areas of Fig. 2, a full discussion of which is beyond the scope of this paper but can be found elsewhere (e.g., Sweby, 1984; Datta-Gupta et al., 1991; Blunt and Rubin, 1992). The Leonard TVD scheme where $\Phi(r) = 2/3 + r/3$ subject to the limiters shown in Fig. 2 has proven robust and accurate (Datta-Gupta et al., 1991) and we adopt it for the applications presented here.

Table 1. Higher-order differencing schemes.

$\Phi(r)$	interface approximation
0	full upstream weighting
1	weighted average
r	two-point upstream
$\frac{(r+1)}{(1+r)}$	Van Leer scheme
$2/3 + r/3$	Leonard scheme

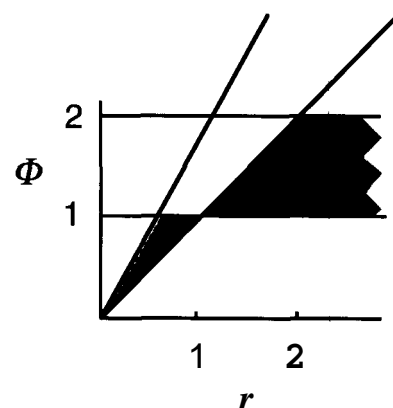


Fig. 2. Shaded region shows values of $\Phi(r)$ for which the higher-order differencing schemes are TVD.

We implemented higher-order differencing schemes in a module based on EOS7R (Oldenburg and Pruess, 1995) of the TOUGH2 (Pruess, 1991) reservoir simulator for two-dimensional rectangular non-uniform grids. Within a TOUGH2 simulation, using higher-order TVD schemes entails finding the upstream grid block, assuming locally one-dimensional flow, calculating $\Phi(r)$, applying the limiters to ensure $\Phi(r)$ is in the TVD region of Fig. 2, and approximating interface values of temperature, concentration, or saturation accordingly. In the case of saturation in TOUGH2, it is actually the relative permeability that is more accurately calculated at interfaces when using higher-order differencing.

VERIFICATION

We have verified our implementation of the Leonard TVD scheme by comparison with a two-dimensional single-phase transport problem for which an analytical solution has been published (Javandel et al., 1984). The problem involves the unidirectional advection of tracer from a line source between 0 and -0.5 m on the left-hand side (see Figs. 3 and 4) and its advection and diffusion in two dimensions. The discretization has uniform square grid blocks 0.10 m on a side with two columns of narrow inactive grid blocks on the left and right-hand sides for a total of 40 by 72 grid blocks. With diffusivity of $1.162 \times 10^{-8} \text{ m}^2 \text{ s}^{-1}$, pore velocity of 0.1 m/day, and grid block size 0.10 m, the cell Peclet number for the problem is approximately 10.

Shown in Figs. 3 and 4 are computed results at $t = 20$ days using upstream weighting and the Leonard TVD scheme, respectively. Comparisons to the analytical solution are presented as profiles along the sections marked AA', BB', and CC' and are shown in Figs. 5, 6, and 7. One can see from these results the improvement obtained by using the Leonard TVD scheme relative to full upstream weighting.

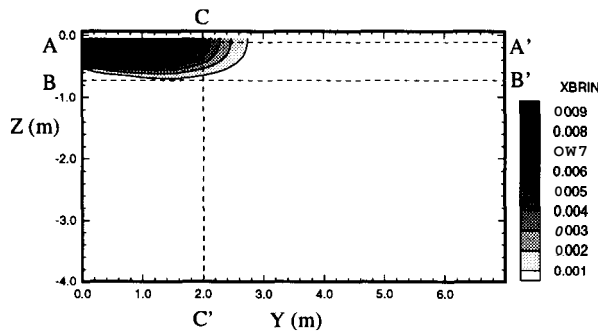


Fig. 3. Tracer plume contours at $t = 20$ days computed using upstream weighting. The cross section lines AA', BB', and CC' are shown.

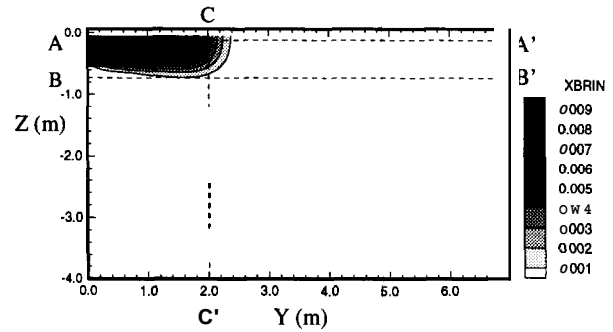


Fig. 4. Tracer plume contours at $t = 20$ days computed using the Leonard TVD scheme. The cross section lines AA', BB', and CC' are shown.

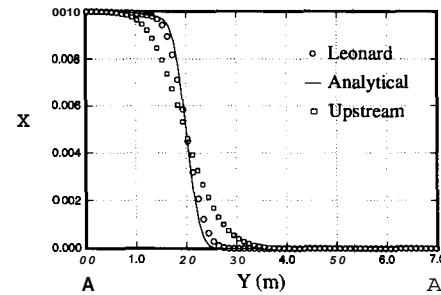


Fig. 5. Comparison of Leonard TVD scheme, analytical, and upstream weighting results for cross section AA'.

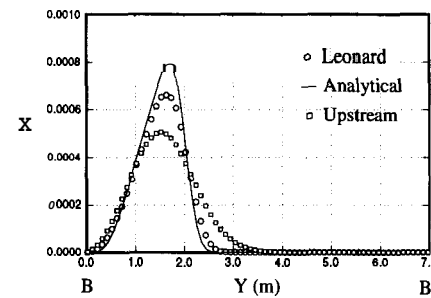


Fig. 6. Comparison of Leonard TVD scheme, analytical, and upstream weighting results for cross section BB'.

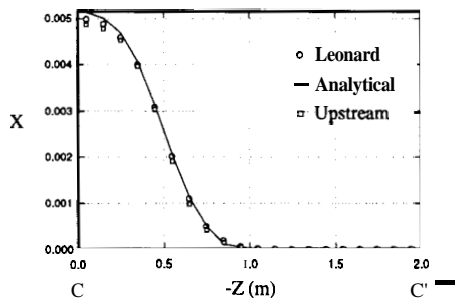


Fig. 7. Comparison of Leonard TVD scheme, analytical, and upstream weighting results for cross section CC'.

APPLICATION

We demonstrate application of the Leonard TVD scheme in **TOUGH2/EOS7R** to a test case involving injection into and production from a two-dimensional sub-horizontal fracture zone. Problem specifications are similar to a production/injection problem previously studied by Pruess (1983) and Pruess and Wu (1993). Production and injection wells are arranged in a five-spot pattern with 400 m well spacing (Fig. 8). Cold water ($T \approx 30$ °C) is injected at a rate of 16 kg/s (full-well basis), and production occurs at the same rate. Four kg of tracer is injected over a period of 10 days starting at $t = 0$. For simplicity we model one quarter of the five-spot pattern, which was discretized into 400 square grid blocks (20 x 20) of length 10 m on a side.

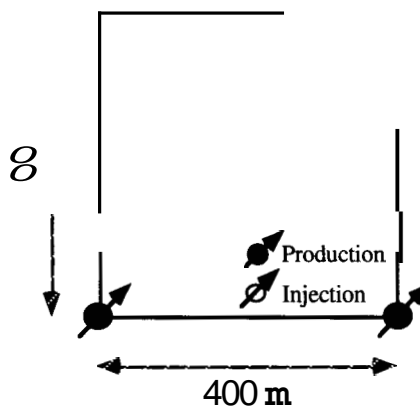


Fig. 8. Five-spot well pattern, with shading showing a 1/4 symmetry element.

The reservoir rock adjacent to the fracture zone is assumed impermeable, and at a uniform initial temperature of 300 °C. Conductive heat transfer to the fracture is modeled with the semi-analytical technique of Vinsome and Westerveld (1980). Boiling occurs near the production well as pressures decline, while cooling occurs at the injection end due to the injection of cold water. We use the module EOS7R

(Oldenburg and Pruess, 1995) for components water, brine, tracer1, tracer2, air, and heat. For this preliminary application, the tracer is the brine component which is non-sorbing, non-decaying, and non-volatilizing although EOS7R is capable of handling all of these processes for the tracer1 and tracer2 components. Parameters for the problem are presented in Table 2.

Table 2. Parameters for injection problem.

Formation	
Thickness of fracture zone	12.2 m
Rock grain density (ρ_R)	2650 kg m ⁻³
Specific heat (c_R)	1000 J kg ⁻¹ °C ⁻¹
Thermal conductivity	2.1 W m ⁻¹ °C ⁻¹
Porosity (ϕ)	0.50
Permeability	1 x 10 ⁻¹² m ²
Relative permeability: Corey curves with	$S_{lr} = 0.30$, $S_{gr} = 0.05$
Tortuosity	1.0
Initial temperature	300 °C
Initial liquid saturation	0.99
Initial pressure	85.93 bar
Production/Injection	
Pattern area	400 m x 400 m
Production rate	16 kg s ⁻¹
Injection rate	16 kg s ⁻¹
Injection enthalpy	125 kJ kg ⁻¹
Tracer injection rate	4.63x10 ⁻⁶ kg s ⁻¹
Tracer injection period	10 days
Molecular diffusivity of tracer	1 x 10 ⁻⁸ m ² s ⁻¹

Results after 6 months computed using upstream weighting for phase saturations, component mass fractions, and thermal energy are shown in Fig. 9. The temperature field shows the effects of cold injection fluid entering the system but being retarded by heat conduction from the reservoir rocks. The tracer mass fraction field is advanced relative to heat since no retarding effects (e.g., adsorption) are present for the tracer. The saturation field shows the development of a two-phase region due to lower pressure at the production well. The final plot gives breakthrough curves of temperature and tracer mass fraction at the production well. Initial tracer breakthrough occurs at about 6 months ($t \approx 1.6 \times 10^7$ s). The retardation of the thermal front is largely masked by cooling due to boiling at the production well. In the absence of induced boiling, thermal breakthrough would be retarded by a factor of (Bodvarsson, 1972)

$$R = \frac{\phi \rho_w c_w}{\phi \rho_w c_w + (1 - \phi) \rho_R c_R} \approx .55 \quad (6)$$

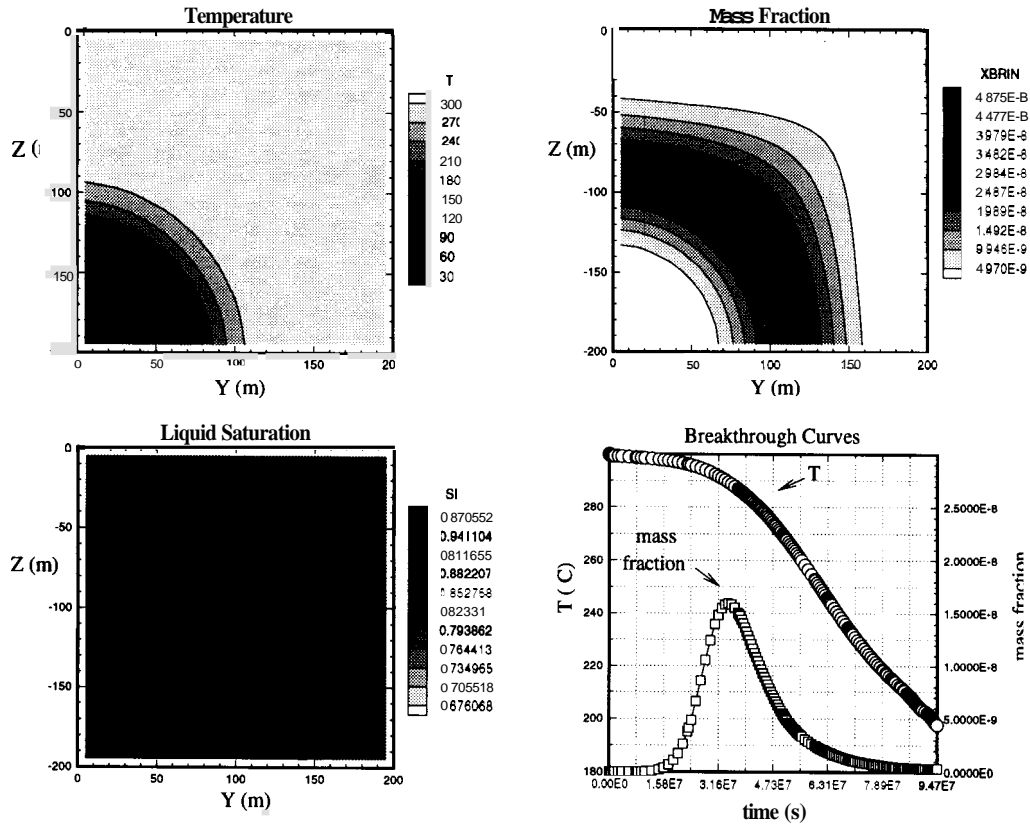


Fig. 9. Results at six months calculated using upstream weighting for two-dimensional geothermal reinjection.

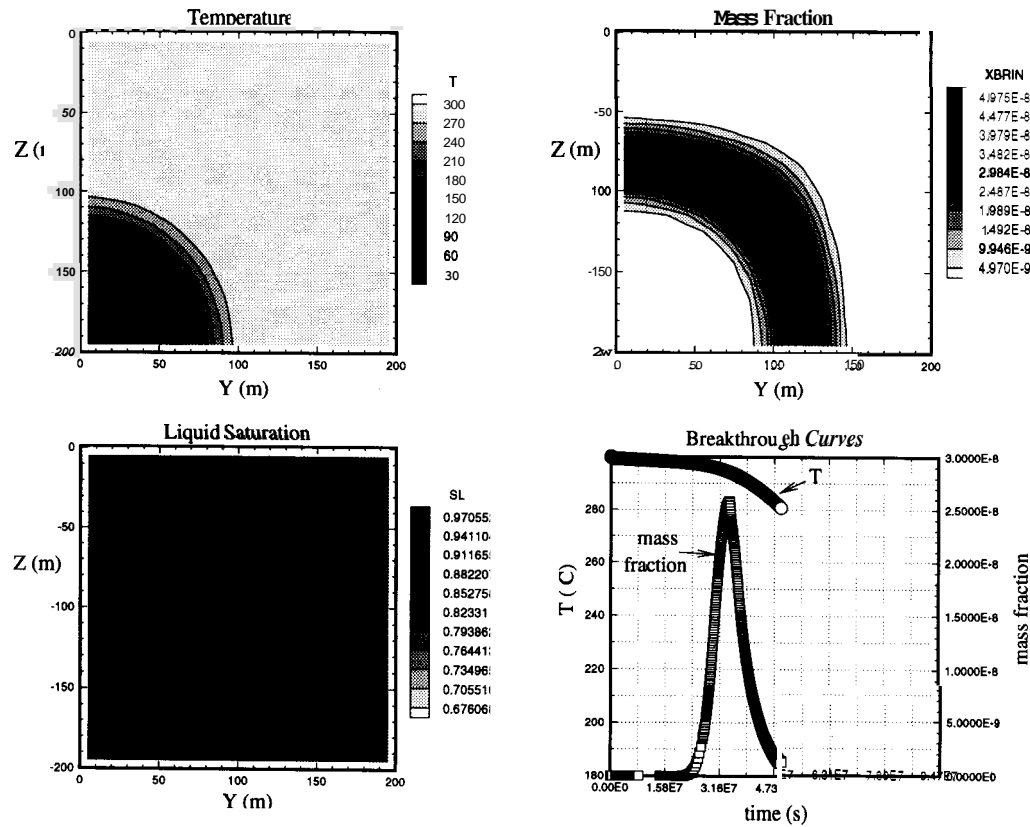


Fig. 10. Results at six months calculated using the Leonard TVD scheme for geothermal reinjection. The breakthrough curve shows the run was stopped after the tail of the tracer pulse was detected.

where we use $\rho_w = 800 \text{ kg m}^{-3}$, $c_w = 4000 \text{ J kg}^{-1} \text{ }^\circ\text{C}^{-1}$ and values from Table 2. Note the broad region of tracer in the mass fraction plot and the gentle rise and decline of the tracer mass fraction in the breakthrough curve; these smoothing effects are due mostly to numerical dispersion.

Results after 6 months computed using the Leonard TVD scheme for phase saturations, component mass fractions, and thermal energy are presented in Fig. 10. Comparing Figs. 9 and 10 we see generally similar results; however, note the relatively sharper fronts for temperature and especially tracer mass fraction. The phase saturation front has evolved differently using the higher-order scheme and is not as far advanced. The breakthrough curves highlight the differences in the schemes. Note the higher maximum and steeper limbs of the tracer breakthrough. Tracer would first be detected at significant concentrations after about 9 months. This sharper tracer breakthrough curve would allow a more accurate prediction of the arrival of the thermal front than the result computed using upstream weighting.

TOUGH2 uses an adaptive time stepping scheme. It is apparent from the symbol spacing in the breakthrough curves in Figs. 9 and 10 that more time steps are needed when using the higher-order scheme. Shorter time steps arise in this problem for two reasons: (1) the sharper front produces larger primary variable changes in grid blocks near the front; and (2) we did not include the dependence of the upstream grid block into the Jacobian matrix for the Newton-Raphson iteration. Because the Jacobian is less accurate, the convergence rate is reduced and the time-step size remains smaller than it would for a more accurate Jacobian matrix.

ICI ONS

The Leonard TVD higher-order differencing scheme was implemented into TOUGH2/EOS7R and verified against a two-dimensional convection-diffusion problem. This new capability was then applied to a geothermal reinjection problem. Sharper profiles of temperature and mass fraction were obtained relative to upstream weighting. Breakthrough curves for the reinjection problem show the improvement in accuracy that can be obtained by using the Leonard TVD scheme. Time-step sizes remain smaller when using the higher-order scheme requiring longer execution times. Part of this limitation on time-step size can be lifted by including the full dependence on upstream grid blocks into the Jacobian.

ACKNOWLEDGMENT

We thank Akhil Datta-Gupta for encouragement in this ongoing project and Stefan Finsterle and Yu-Shu Wu for careful reviews. This work was supported by the Assistant Secretary for Energy Efficiency and

Renewable Energy, Geothermal Division, U.S. Department of Energy, under contract No. DE-AC03-76SF00098.

REFERENCES

- Blunt, M., and B. Rubin, Implicit flux limiting schemes for petroleum reservoir simulation, *J. Comput. Physics*, **102**, 194–210, 1992.
- Bodvarsson, G. Thermal Problems in the Siting of ReInjection Wells, *Geothermics*, **1(2)**, 63-66, 1972.
- Datta-Gupta, A., L.W. Lake, G. A. Pope, and K. Sepehnoori, High-resolution monotonic schemes for reservoir fluid flow simulation, *In Situ*, **15(3)**, 289–317, 1991.
- Javandel, I., C. Doughty, and C.F. Tsang, *Groundwater Transport: Handbook of mathematical models*, Am. Geophys. Union Water Resources Monograph 10, 1984.
- Leonard, B.P., Third-order upwinding as a rational basis for computational fluid dynamics, in *Computational Techniques and Applications*, Elsevier Science Publishers, North-Holland, 1984.
- Liu, J., G.A. Pope, and K. Sepehnoori, A high-resolution, fully implicit method for enhanced oil recovery simulation, *SPE-29098*, presented at the SPE Symposium on Reservoir Simulation held in San Antonio TX 12–15 February 1995.
- Oldenburg, C.M. and K. Pruess, EOS7R: Radionuclide Transport for TOUGH2, Lawrence Berkeley National Laboratory Report *LBL-34868*, November 1995.
- Pruess, K., TOUGH2- A general-purpose numerical simulator for multiphase fluid and heat flow, Lawrence Berkeley National Laboratory Report *LBL-29400*, May 1991.
- Pruess, K., Heat transfer in fractured geothermal reservoirs with boiling, *Water Resources Research*, **19(1)**, 201–208, 1983.
- Pruess, K., and Y.-S. Wu, A new semi-analytical method for numerical simulation of fluid and heat flow in fractured reservoirs, *SPE Advanced Technology Series*, **1(2)**, 63–72, 1993.
- Sweby, P.K., High resolution schemes using flux limiters for hyperbolic conservation laws, *SZAM J. Numer. Anal.*, **21(5)**, 995–1011, 1984.
- Vinsome, P. K. W. and J. Westerveld. A Simple Method for Predicting Cap and Base Rock Heat Losses in Thermal Reservoir Simulators, *J. Canadian Pet. Tech.*, **19(3)**, 87–90, July-September 1980.